American Mineralogist, Volume 91, pages 319–326, 2006

Equations of state and structures of andalusite to 9.8 GPa and sillimanite to 8.5 GPa

JASON B. BURT,[1,*] NANCY L. ROSS,[1] ROSS J. ANGEL,[1] AND MARIO KOCH[1,†]

[1]Department of Geosciences, Virginia Polytechnic Institute and State University, Blacksburg, Virginia 24061, U.S.A.

ABSTRACT

The equations of state and structures of andalusite and sillimanite have been determined using high-pressure single-crystal X-ray diffraction. A third-order Birch-Murnaghan equation-of-state fit to 14 *P-V* data points measured between 1 bar and 9.8 GPa for andalusite yields values of K_{T0} = 144.2(7) GPa and K' = 6.8(2). A similar analysis for sillimanite involving a fit to 13 *P-V* data points between 1 bar and 8.5 GPa results in K_{T0} = 164(1) GPa and K' = 5.0(3). The axial compression of both structures is nonlinear and highly anisotropic (~60%) with the *c*-axis being the least compressible axis in both structures. The axial moduli determined with a parameterized form of the third-order Birch-Murnaghan equation of state are: K_{a_0} = 163(1) GPa, K_{b_0} = 113.1(7) GPa, and K_{c_0} = 297(1) GPa with K'_{a_0} = 2.1(3), K'_{b_0} = 5.08(19), and K'_{c_0} = 11.1(4) for sillimanite, and K_{a_0} = 99.6(7) GPa, K_{b_0} = 152.2(9) GPa, and K_{c_0} = 236(3) GPa with K'_{a_0} = 5.83(19), K'_{b_0} = 7.6(3), and K'_{c_0} = 5.5(9) for andalusite. The major compression mechanism in both structures involves shortening of bond lengths within the AlO_6 octahedra with volume reductions of 7.4% and 5.1% in sillimanite and andalusite, respectively, over the pressure ranges studied. In andalusite there is also significant compression of the AlO_5 polyhedra and, to a lesser degree, the SiO_4 tetrahedra that display reductions of 5.0% and 3.1% in volume, respectively. In sillimanite there is no significant compression of either the AlO_4 or SiO_4 tetrahedra which behave as rigid, incompressible units.

Keywords: Andalusite, sillimanite, high-pressure studies, equation of state, XRD data, single crystal, crystal structure

INTRODUCTION

The Al_2SiO_5 polymorphs kyanite, andalusite, and sillimanite have been extensively studied due to their abundance in metapellitic rocks and their use as thermobarometers (e.g., Kerrick 1990). The polymorphs are also of interest because their crystal structures can accommodate aluminum in four-, five-, and sixfold coordination with oxygen. In sillimanite, for example, an orthorhombic polymorph with space group *Pbnm*, half of the aluminum is found in edge-sharing octahedral chains that run parallel to [001] with adjacent tetrahedral chains consisting of alternating tetrahedral AlO_4 and SiO_4 groups (Fig. 1a). Andalusite is also orthorhombic (space group *Pnnm*) and, similar to sillimanite, one-half of the aluminum atoms occupy chains of AlO_6 running parallel to [001]. However, the other half occurs in AlO_5 polyhedra which are cross-linked by SiO_4 tetrahedra (Fig. 1b).

Accurate equation-of-state measurements for minerals such as the Al_2SiO_5 polymorphs are important because they provide vital input for thermodynamic databases from which phase equilibria can be calculated. The equation of state of sillimanite was examined by Yang et al. (1997) using single-crystal X-ray diffraction and by Friedrich et al. (2004) using synchrotron powder X-ray diffraction (Table 1). These studies determined isothermal bulk moduli, K_{T0}, of 171(7) GPa and 176(11) GPa, respectively, from *P-V* data collected to 5.29 GPa (Yang et al. 1997) and 46 GPa (Friedrich et al. (2004). In both studies, the pressure derivative of the bulk modulus, K', could not be constrained and was assumed to be equal to four. Yang et al. (1997) also reanalyzed Ralph et al.'s (1984) *P-V* data for andalusite that was collected to 3.7 GPa and determined that K_{T0} = 151(3) GPa (also with K' constrained to be 4), contrasting with the original determination of K_{T0} = 135(10) GPa. It should be noted that the study of Ralph et al. (1984) was one of the first high-pressure studies of a single crystal in a diamond anvil cell (DAC) using X-ray diffraction. Vaughan and Weidner (1978) determined the adiabatic bulk modulus, K_S, from Brillouin spectroscopy measurements of andalusite and sillimanite to be 158 GPa and 166 GPa (Reuss bound values), respectively. Theoretical calculations of the bulk modulus for andalusite and sillimanite have also been reported by Matsui (1996), Oganov et al. (2001), and Winkler et al. (2001). Matsui (1996) reported a bulk modulus of 175 GPa for sillimanite and 104 GPa for andalusite based on molecular dynamics calculations. Oganov et al. (2001) calculated the bulk moduli of andalusite and sillimanite to be 145.3 and 160.1 GPa with K' values of 3.88 and 2.69, respectively, using the VASP (Vienna Ab Initio Simulation Package) program, while Winkler et al. (2001) calculated bulk moduli of andalusite and sillimanite to be 145 and 159 GPa, respectively, using the CASTEP (CAmbridge Serial Total Energy Package) program.

Even though these polymorphs have been extensively studied, it is clear from the preceding discussion that there is a considerable spread in the values of K_{T0}, especially for andalusite. In addition, the previous X-ray diffraction experiments of both polymorphs assumed K' = 4. Recent improvements in determining both the volume and pressure in single-crystal X-ray

* E-mail: jaburt@vt.edu
† Present address: Univ. of Heidelberg, Inst. Mineral., Heidelberg, D-69120 Germany.

TABLE 1. Isothermal bulk moduli, K_{T0}, of andalusite and sillimanite

Andalusite				Sillimanite			
Method	K_{T0} (GPa)	K'	Ref.	Method	K_{T0} (GPa)	K'	Ref.
XRD (single crystal)	144.2(7)	6.8(2)	(7)	XRD (single crystal)	164(1)	5.0(3)	(7)
XRD (single crystal)	135(10)	4	(1)	XRD (single crystal)	171(7)	4	(2)
XRD (single crystal)	151(3)	4	(2)	XRD (Powder)	176(11)	4	(6)
Brillouin (Reuss)	158		(3)	Brillouin (Reuss)	166.4		(3)
Brillouin (Voigt)	165.9		(3)	Brillouin (Voigt)	175.1		(3)
Theoretical (DFT)	145.3	3.88	(4)	Theoretical (DFT)	160.1	2.69	(4)
Theoretical (DFT)	143.5	4	(4)	Theoretical (DFT)	148	4	(4)
Theoretical (DFT)	145		(5)	Theoretical (DFT)	159		(5)
Theoretical (THB)	191		(5)	Theoretical (THB)	198		(5)

Notes: (1) Ralph et al. (1984); (2) Yang et al. (1997); (3) Vaughan and Weidner (1978); (4) Organov et al. (2001); (5) Winkler et al. (2001); (6) Friedrich et al. (2004); (7) this study.

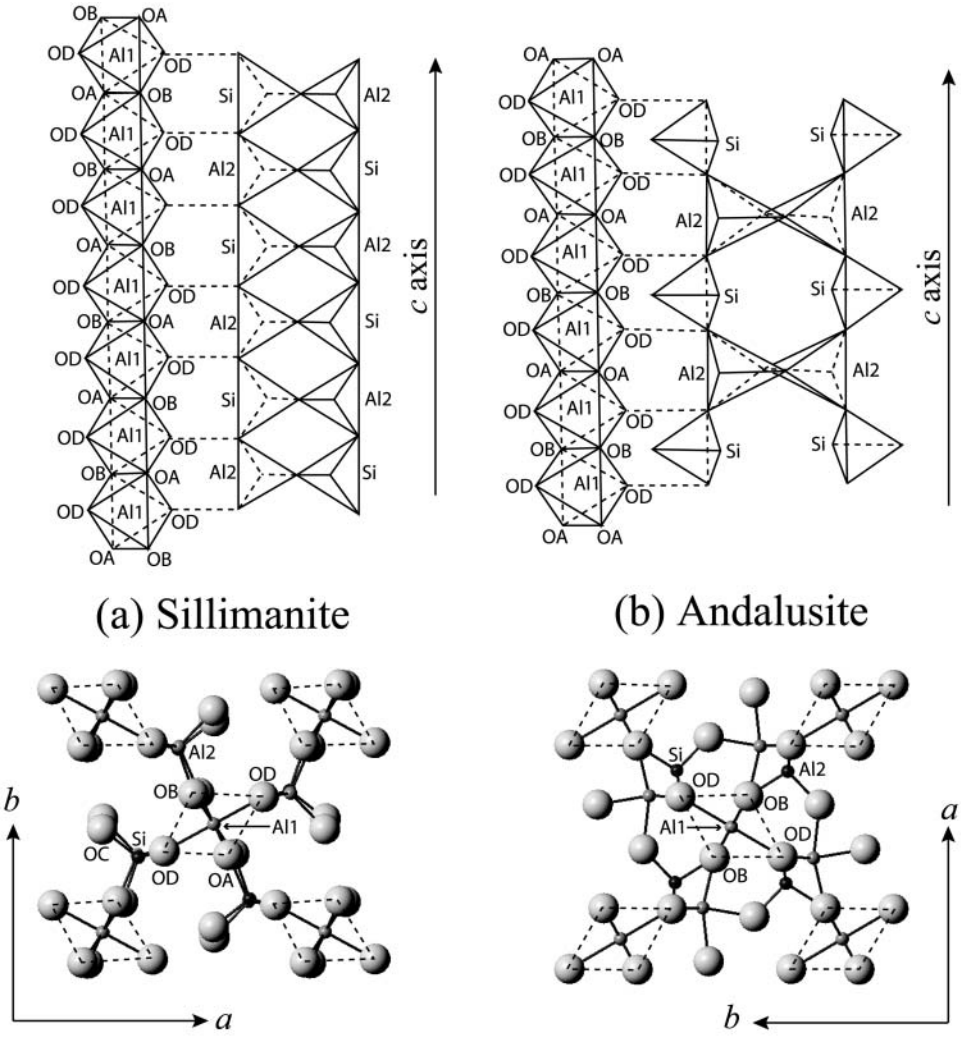

FIGURE 1. Projection of the alternating aluminum and silica polyhedra backbone down *c* and projection of the structures of (**a**) sillimanite and (**b**) andalusite on to (001).

experiments allow more precise determinations of equations of state (Angel 2001). Provided one has good quality single crystals, volumes of single crystals loaded in diamond anvil cells (DACs) can be measured to better than 1 part in 10000. Bulk moduli can be determined with e.s.d. values of 1% or less and accurate values of K' can also be determined (e.g., Angel 2001). Such high-pressure single-crystal X-ray diffraction experiments have shown that the assumption that $K' = 4$ is not valid for many minerals. We report here the equations of state and high-pressure structural behavior of andalusite and sillimanite. The structural studies provide information about the compressional mechanisms and their influence on the equation of state. We address the ques-

tions of whether a second-order Birch-Murnaghan equation of state is valid for andalusite and sillimanite, what structural features control compression of the two structures, whether the compression mechanisms are similar, and how these affect the overall changes in the distortion of the structures. In addition, this study extends the previous pressure ranges of high-pressure single-crystal X-ray diffraction studies from 3.7 to 9.8 GPa for andalusite and 5.29 to 8.54 GPa for sillimanite.

Experimental methods

The sillimanite sample was kindly provided by Carl Francis, curator of the Harvard mineral collection, and is from the Okkamitiya Sabaragamuiwa province of Sri Lanka (sample no. 131013). The andalusite sample is from Minas Gerais, Brazil, and was obtained from a gem dealer in Idar Oberstein, Germany. An andalusite crystal measuring 272 × 112 × 56 μm and a sillimanite crystal measuring 130 × 112 × 30 μm were picked based on their optical quality and X-ray diffraction peak profiles. Each crystal was loaded in an ETH-type diamond anvil cell (Miletich et al. 2000) along with a quartz crystal and a ruby chip for pressure calibration. Unit-cell parameters were obtained from a Huber four-circle diffractometer using Mo$K\alpha$ radiation (λ = 0.7107 Å) with a tube power of 50 kV and 40 mA. The room-pressure unit-cell parameters were collected in the DAC without fluid, while the high-pressure data were collected using a 4:1 mixture of methanol:ethanol as the pressure-transmitting medium. Tungsten was initially used as the gasket material up to pressures of 6.5 GPa for andalusite and 6.3 GPa for sillimanite before deformation of the gasket hindered further increases in pressure. The gaskets were replaced with T301 steel and, in the case of andalusite, a gasket prepared with a 304 μm diameter hole and thickness of 80 μm remained stable up to 9.8 GPa. The unit-cell parameters (Tables 2 and 3) were calculated using a vector least squares fit of 22–35 reflections between 9° and 27° 2θ for andalusite and between 11° and 32° 2θ for sillimanite centered at 8 equivalent positions following the procedure of King and Finger (1979). The initial unconstrained unit-cell refinements did not deviate from orthorhombic symmetry for either crystal throughout the pressure range studied. The volume of a quartz crystal within the diamond anvil cell was used to determine the pressure from the third-order Birch-Murnaghan equation of state of quartz: K_{T0} = 37.12(9) GPa and K_0' = 5.99(4) (Angel 1997). Equation-of-state parameters of andalusite and sillimanite were obtained by a weighted-least-squares fit of the Birch-Murnaghan 3rd-order equation of state to the *P-V* data using the program EosFit 5.2 (Angel 2001).

X-ray intensity data for andalusite were collected at 0.0001, 1.474(5), 2.512(6), 3.129(6), 3.932(7), 5.441(6), 7.565(8), and 9.828(9) GPa and at 0.0001, 1.548(5), 4.144(7), 5.750(7), and 7.663(8) GPa for sillimanite using an Oxford Diffraction Xcalibur single-crystal X-ray diffractometer with monochromatized Mo$K\alpha$ radiation (λ = 0.70923 Å), tube power of 50 kV and 40 mA, and a point detector. The data sets were collected using the fixed Φ mode from 4° to 40° in θ for both samples with an omega scan of 0.05° per second, scan width of 1.2° and a step number of 60 for andalusite and an omega scan of 0.02° per second, scan width of 1.2° and a step number of 60 for sillimanite. The peaks were integrated using the program Win-IntegrStp v3.4 (Angel 2003) that performs a full peak-profiling of the step-scan data based on the methods of Pavese and Artioli (1996). Absorption corrections for the integrated intensities were made using ABSORB 6.0 (Angel 2004; Burnham 1966) that corrects for absorption by the crystal, components of the DAC, and for gasket shadowing. Overall transmission through the DAC ranged from 0.16 to 0.37 for andalusite and 0.22 to 0.25 for sillimanite. Symmetrically equivalent reflections for both crystals were averaged in Laue group *mmm* and R(int) values are given in Tables 4 and 5.

The crystal-structure refinements were carried out with RFINE99, developed from a previous version, RFINE4 (Finger and Prince 1974). Initial atomic coordinates for andalusite and sillimanite were taken from Winter and Ghose (1979) and atomic scattering factors and coefficients for dispersion correction from the *International Tables for Crystallography* (Maslen et al. 1992; Creagh and McAuley 1992). Details of the refinements are given in Tables 4 and 5, the refined atomic positions and displacement parameters are given in Tables 6 and 7, and selected interatomic distances and angles for sillimanite and andalusite are given in Tables 8 and 9, respectively.

Table 2. Unit-cell parameters of sillimanite, space group *Pbnm*, from 1 bar to 8.543 GPa

Pressure (GPa)	*a*-axis (Å)	*b*-axis (Å)	*c*-axis (Å)	Volume (Å³)
0.0001	7.48388(17)	7.6726(3)	5.76807(13)	331.208(18)
0.239(4)	7.48009(16)	7.6672(4)	5.76652(12)	330.71(2)
1.016(4)	7.46853(12)	7.6507(3)	5.76169(9)	329.220(14)
1.548(5)	7.46040(15)	7.6395(4)	5.75840(12)	328.190(19)
2.292(5)	7.44882(12)	7.6235(2)	5.75396(9)	326.745(13)
3.431(6)	7.43271(11)	7.6011(3)	5.7472(1)	324.694(13)
3.747(5)	7.42883(18)	7.5952(3)	5.74536(11)	324.150(17)
4.144(7)	7.42183(13)	7.5868(3)	5.74298(11)	323.375(16)
4.685(6)	7.41448(12)	7.5771(3)	5.74011(9)	322.479(13)
5.750(7)	7.39939(11)	7.5576(2)	5.73421(8)	320.667(11)
6.348(7)	7.39134(12)	7.5475(2)	5.73114(9)	319.717(13)
7.663(8)	7.3717(2)	7.5243(4)	5.72421(11)	317.503(19)
8.543(8)	7.36058(12)	7.5106(2)	5.72007(8)	316.221(12)

Note: The figures in parentheses represent 1 e.s.d. of last decimal place shown.

Table 3. Unit-cell parameters of andalusite, space group *Pnnm*, from 1 bar to 9.828 GPa

Pressure (GPa)	*a*-axis (Å)	*b*-axis (Å)	*c*-axis (Å)	Volume (Å³)
0.0001	7.7930(3)	7.89734(17)	5.55583(14)	341.926(15)
0.605(4)	7.7780(4)	7.8868(2)	5.5513(2)	340.54(2)
1.474(5)	7.7568(3)	7.87268(18)	5.54488(15)	338.607(16)
2.265(5)	7.7381(3)	7.8602(2)	5.53919(18)	336.908(19)
2.512(6)	7.7320(3)	7.85659(16)	5.53642(16)	336.320(16)
3.129(6)	7.7186(4)	7.8467(2)	5.5329(2)	335.10(2)
3.932(7)	7.7014(3)	7.8354(2)	5.52629(17)	333.472(18)
4.586(7)	7.6877(3)	7.82600(17)	5.52187(15)	332.219(15)
5.051(7)	7.6783(4)	7.8197(2)	5.51841(18)	331.336(19)
5.441(6)	7.6704(3)	7.81452(18)	5.51589(16)	330.625(16)
6.516(8)	7.6494(5)	7.7997(3)	5.5085(2)	328.65(3)
7.565(8)	7.6313(3)	7.78625(19)	5.50175(14)	326.910(14)
8.465(8)	7.6145(4)	7.7753(2)	5.49544(18)	325.358(19)
9.828(9)	7.5922(8)	7.7600(5)	5.4872(4)	323.28(4)

Note: The figures in parentheses represent 1 e.s.d. of last decimal place shown.

Results and discussion

The variation of volume with pressure of sillimanite and andalusite is shown in Figure 2. No phase transitions are observed in either polymorph over the pressure range studied. A third-order Birch-Murnaghan equation-of-state fit to the *P-V* data yields values of V_o = 331.214(18) Å³, K_{T0} = 164(1) GPa, and K' = 5.0(3) for sillimanite and V_o = 341.940(16) Å³, K_{T0} = 144.2(7) GPa, and K' = 6.8(2) for andalusite. The equation-of-state data is weighted based on uncertainties in pressure and volume using the effective variance method (Orear 1982). The largest difference among the observed and calculated pressures is 0.043 GPa for sillimanite and 0.040 GPa for andalusite. The weighted

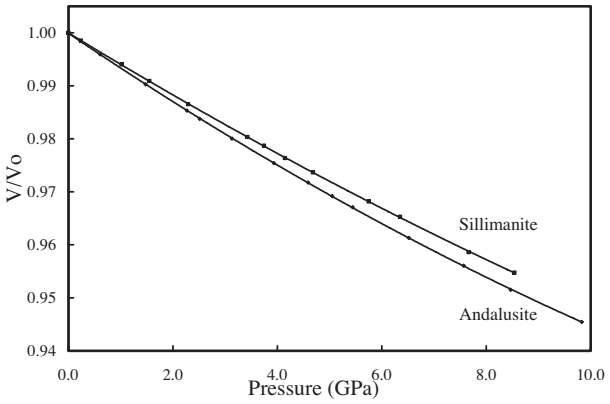

Figure 2. Variation of the unit-cell volume of andalusite (diamonds) between room pressure and 9.8 GPa and for sillimanite (squares) between room pressure and 8.6 GPa. The esd's are smaller than the symbols shown and the lines are the EoS fit to the data.

TABLE 4. Details of least-squares structure refinements for sillimanite at room pressure through 7.663 GPa

Pressure (GPa)	0.0001	1.548(5)	4.144(7)	5.750(7)	7.663(8)
ρ_{calc} (g/cm^3)	3.249	3.29	3.343	3.356	3.39
μ (mm^{-1})	1.123	1.137	1.155	1.159	1.171
Θ range for data collection	4° ~ 40°	4° ~ 40°	4° ~ 40°	4° ~ 40°	4° ~ 40°
Limiting Indices	$-13 \le h \le 13$, $-2 \le k \le 2$, $-10 \le l \le 10$	$-13 \le h \le 11$, $-2 \le k \le 3$, $-9 \le l \le 10$	$-11 \le h \le 12$, $-2 \le k \le 2$, $-9 \le l \le 10$	$-10 \le h \le 12$, $-2 \le k \le 2$, $-10 \le l \le 10$	$-13 \le h \le 10$, $-2 \le k \le 2$, $-9 \le l \le 9$
No. refl. >2 $I_o/\sigma(I_o)$	837	845	764	776	696
No. ind. Refl. [$F > 2\sigma(F)$]	180	195	171	158	156
R_{int}*	0.038(166)	0.041(180)	.049(160)	0.041(140)	0.046(147)
No. of paramters	22	22	22	22	22
G_{fit}†	1.17	1.32	1.11	1.23	1.23
Extinction Factor ($\times 10^{-4}$)	0.19(5)	0.29(5)	0.24(5)	0.36(6)	0.16(5)
R_w‡§	0.029(173)	0.038(188)	0.039(168)	0.040(150)	0.037(144)
R||§	0.026(173)	0.034(188)	0.035(168)	0.035(150)	0.033(144)

* Internal residual on F (number of averaged reflections).
† G_{fit} = estimated standard deviation of unit weight observation.
‡ $R_w = (\Sigma w(|F_o| - |F_c|)^2/\Sigma|F_o|^2]^2$.
§ Number of reflections used in refinement are in parentheses.
|| $R = \Sigma||F_o| - |F_c||/\Sigma|F_o|$.

TABLE 5. Details of least–squares structure refinements for andalusite at room pressure through 9.828 GPa

Pressure (GPa)	0.0001	1.474(5)	2.512(6)	3.129(6)	3.932(7)	5.441(6)	7.565(8)	9.828(9)
ρ_{calc} (g/cm^3)	3.147	3.178	3.2	3.212	3.227	3.255	3.292	3.329
μ (mm^{-1})	1.087	1.098	1.106	1.11	1.115	1.125	1.137	1.15
θ range for data collection	4° ~ 40°	4° ~ 40°	4° ~ 40°	4° ~ 40°	4° ~ 40°	4° ~ 40°	4° ~ 40°	4° ~ 40°
Limiting Indices	$-5 \le h \le 6$, $-12 \le k \le 12$, $-9 \le l \le 9$	$-5 \le h \le 5$, $-12 \le k \le 12$, $-9 \le l \le 9$	$-5 \le h \le 6$, $-12 \le k \le 12$, $-9 \le l \le 9$	$-5 \le h \le 5$, $-12 \le k \le 13$, $-9 \le l \le 9$	$-5 \le h \le 6$, $-12 \le k \le 13$, $-9 \le l \le 9$	$-5 \le h \le 5$, $-12 \le k \le 12$, $-9 \le l \le 9$	$-9 \le h \le 9$, $-9 \le k \le 9$, $-9 \le l \le 9$	$-9 \le h \le 9$, $-9 \le k \le 9$, $-9 \le l \le 9$
No. refl. >2 $I_o/\sigma(I_o)$	937	1020	967	1054	905	935	811	919
No. ind. Refl. [$F > 2\sigma(F)$]	282	300	305	322	270	297	285	270
R_{int}*	0.051(259)	0.042(269)	0.037(271)	0.037(280)	0.042(246)	0.043(271)	0.044(226)	0.063(252)
No. of paramters	22	22	22	22	22	22	22	22
G_{fit}†	1.21	1.31	1.45	1.33	1.4	1.39	1.23	1.2
Extinction Factor (x10^{-4})	0.15(7)	0.22(5)	0.16 (5)	0.18(5)	0.36(6)	0.17(5)	0.16 (5)	0.09(6)
R_w‡§	0.043 (275)	0.039 (294)	0.041 (294)	0.037 (308)	0.045 (264)	0.043(286)	0.044 (272)	0.05 (250)
R||§	0.032 (275)	0.031 (294)	.0.34 (294)	0.030 (308)	0.038 (264)	0.036 (286)	0.039 (272)	0.043 (250)

* Internal residual on F (number of averaged reflections).
† G_{fit} = estimated standard deviation of unit weight observation.
‡ $R_w = [\Sigma w(|F_o| - |F_c|)^2/\Sigma|F_o|^2]^2$.
§ Number of reflections used in refinement are in parentheses.
|| $R = \Sigma||F_o| - |F_c||/\Sigma|F_o|$.

chi-squared values, $\chi^2_w = 2.65$ for sillimanite and $\chi^2_w = 1.58$ for andalusite, suggest that the errors in volume and/or pressure may have been underestimated in sillimanite. The results from this study show that sillimanite is 12% less compressible than andalusite. These EoS parameters are fortuitously close to those determined by Oganov et al. (2001) and Winkler et al. (2001). Although the bulk moduli determined by Organov et al. (2001) are similar to those determined in this study the K' values are significantly different. Vaughan and Weidner (1978) determined K_S of andalusite and sillimanite from Brillouin experiments and, while the K_S of sillimanite is similar to K_{TO} determined in this study, the K_S of andalusite is ~10% higher. Previous high-pressure single-crystal X-ray diffraction studies of andalusite and sillimanite determined higher K_{TO} values as a result of K' being constrained to be equal to 4 (Yang et al. 1997).

The difference in K' can best be seen in a plot of normalized stress, F_e, against Eulerian finite strain, f_e (Fig. 3). The slope of a line fit to data in an F-f plot reflects the value of K', while the intersection of the line with the normalized stress axis corresponds to the bulk modulus at room temperature. An equation of state with K' equal to 4 would be a horizontal line in a F-f plot while those with values of $K' > 4$ would have positive slopes and those with $K' < 4$ would have negative slopes (Angel 2001). It is clear from Figure 3 that andalusite has a K' significantly greater than 4 and that sillimanite has a K' slightly greater than 4, showing that a second-order Birch-Murnaghan equation of state is not an adequate description of the P-V data. Indeed, a second-order Birch-Murnaghan equation-of-state results in significantly worse

TABLE 6. Positional and isotropic displacement parameters for sillimante at 1 bar through 7.663 GPa

		0.0001	1.548(5)	4.144(7)	5.750(7)	7.663(8)
Al1	B_{iso}	0.33(2)	0.40(3)	0.41(3)	0.28(4)	0.25(3)
Al2	x	0.14181(13)	0.14164(15)	0.1411(17)	0.14001(19)	0.1397(2)
	y	0.3451(5)	0.3439(7)	0.3410(7)	0.3378(8)	0.3389(7)
	B_{iso}	0.40(2)	0.49(3)	0.47(3)	0.31(4)	0.32(4)
Si	x	0.15318(12)	0.15356(14)	0.15455(16)	0.15466(17)	0.1550(2)
	y	0.3407(5)	0.3414(6)	0.3377(7)	0.3363(7)	0.3363(7)
	B_{iso}	0.39(2)	0.37(3)	0.44(3)	0.28(3)	0.25(4)
OA	x	0.3607(3)	0.3614(3)	0.3629(4)	0.3639(4)	0.3642(5)
	y	0.4075(12)	0.4054(15)	0.4080(15)	0.4142(18)	0.4117(16)
	B_{iso}	0.35(4)	0.41(5)	0.41(6)	0.41(7)	0.22(8)
OB	x	0.3572(3)	0.3562(4)	0.3556(4)	0.3545(4)	0.3550(5)
	y	0.4348(13)	0.4337(16)	0.4364(16)	0.4452(19)	0.4411(18)
	B_{iso}	0.42(4)	0.44(5)	0.48(6)	0.42(7)	0.55(9)
OC	x	0.4762(3)	0.4756(4)	0.4747(4)	0.4738(5)	0.4723(5)
	y	0.0022(12)	0.0040(15)	0.0051(15)	0.0047(16)	0.0033(2)
	B_{iso}	0.94(5)	0.94(7)	0.97(7)	0.85(8)	0.84(8)
OD	x	0.1258(2)	0.1261(3)	0.1267(3)	0.1275(3)	0.1285(3)
	y	0.2228(10)	0.2223(13)	0.2194(12)	0.2162(14)	0.2167(14)
	z	0.5151(2)	0.5148(3)	0.5154(3)	0.5154(4)	0.5148(6)
	B_{iso}	0.54(3)	0.61(4)	0.59(5)	0.47(5)	0.47(6)

Note: General fractional coordinates for the atoms: Al1 (0 0 0), Al2 (x y .25), Si (x y .75), OA (x y .75), OB (x y .25), OC (x y .75), and OD (x y z)

TABLE 7. Positional and isotropic displacement parameters for andalusite at 1 bar through 9.828 GPa

		0.0001	1.474(5)	2.512(6)	3.129(6)	3.932(7)	5.441(6)	7.565(8)	9.828(9)
Al1	*z*	0.2418(2)	0.24198(17)	0.2415(2)	0.24182(14)	0.2419(3)	0.2417(2)	0.2418(2)	0.2418(3)
	B_{iso}	0.44(3)	0.29(2)	0.31(2)	0.299(19)	0.31(3)	0.30(2)	0.30(3)	0.28(3)
Al2	*x*	0.3703(4)	0.3704(2)	0.3700(4)	0.3699(2)	0.3702(6)	0.3695(4)	0.3694(2)	0.3693(3)
	y	0.13879(16)	0.13868(12)	0.13868(11)	0.13831(11)	0.13830(17)	0.13774(14)	0.1378(2)	0.1378(2)
	B_{iso}	0.41(3)	0.31(2)	0.31(2)	0.321(19)	0.31(3)	0.30(2)	0.36(3)	0.28(3)
Si	*x*	0.2465(4)	0.2464(2)	0.2466(3)	0.2466(2)	0.2472(5)	0.2475(3)	0.2471(2)	0.2479(2)
	y	0.25237(15)	0.25148(10)	0.25092(12)	0.25083(9)	0.25020(15)	0.24974(15)	0.2485(2)	0.24784(18)
	B_{iso}	0.40(2)	0.28(2)	0.301(19)	0.294(17)	0.28(2)	0.30(2)	0.37(3)	0.28(3)
OA	*x*	0.4224(7)	0.4217(6)	0.4208(8)	0.4203(5)	0.4215(10)	0.4203(8)	0.4194(5)	0.4187(6)
	y	0.3638(4)	0.3630(3)	0.3637(3)	0.3631(2)	0.3635(4)	0.3633(3)	0.3621(6)	0.3631(5)
	B_{iso}	0.43(5)	0.3159(4)	0.37(4)	0.33(3)	0.35(5)	0.3304(4)	0.39(5)	0.33(6)
OB	*x*	0.4254(7)	0.4257(6)	0.4270(8)	0.4272(5)	0.4259(11)	0.4287(8)	0.4290(5)	0.4309(6)
	y	0.3619(4)	0.3615(3)	0.3608(3)	0.3601(2)	0.3599(4)	0.3584(3)	0.3568(5)	0.3562(5)
	B_{iso}	0.42(5)	0.36(4)	0.34(5)	0.32(3)	0.38(6)	0.33(5)	0.37(6)	0.37(6)
OC	*x*	0.1017(7)	0.1018(6)	0.1044(9)	0.1020(5)	0.1045(12)	0.10377	0.1038(5)	0.1043(5)
	y	0.4012(3)	0.4004(3)	0.4001(3)	0.3998(3)	0.3996(4)	0.3999(3)	0.3990(5)	0.4003(5)
	B_{iso}	0.73(6)	0.70(4)	0.67(5)	0.71(4)	0.70(6)	0.75(5)	0.64(7)	0.77(7)
OD	*x*	0.2292(5)	0.2302(4)	0.2296(6)	0.2296(4)	0.2289(7)	0.2292(5)	0.2291(3)	0.2288(4)
	y	0.1341(2)	0.13261(12)	0.1320(2)	0.13146(17)	0.1315(3)	0.1303(2)	0.1290(3)	0.1285(4)
	z	0.2388(4)	0.2395(3)	0.2400(4)	0.2394(3)	0.2398(4)	0.2399(4)	0.2391(4)	0.2393)4)
	B_{iso}	0.52(4)	0.45(3)	0.47(3)	0.44(3)	0.40(4)	0.39(3)	0.37(4)	0.33(5)

Notes: General fractional coordinates for the atoms: Al1 (0 0 *z*), Al2 (*x y* .5), Si (*x y* 0), OA (*x y* .5), OB (*x y* 0), OC (*x y* 0), and OD (*x y z*).

TABLE 8. Selected bond lengths (Å) and angles (°) for andalusite from 1 bar through 9.828 GPa

Bond or Angle	Pressure (GPa)							
	0.0001	1.474(5)	2.512(6)	3.129(6)	3.932(7)	5.441(6)	7.565(8)	9.828(9)
Al1-OA (x2)	1.824(3)	1.825(2)	1.819(3)	1.823(2)	1.816(4)	1.814(3)	1.817(3)	1.808(3)
Al1-OB (x2)	1.893(3)	1.889(2)	1.888(3)	1.8873(18)	1.888(4)	1.885(3)	1.885(3)	1.878(3)
Al1-OD (x2)	2.076(3)	2.069(3)	2.056(4)	2.050(3)	2.042(5)	2.031(4)	2.016(3)	2.003(3)
AVG.	1.93	1.93	1.92	1.92	1.92	1.91	1.91	1.90
Poly. Vol.	9.49(7)	9.44(6)	9.34(8)	9.34(5)	9.27(9)	9.20(7)	9.15(7)	9.00(7)
OA-Al1-OB	96.70(12)	96.56(9)	96.63(12)	96.45(9)	96.48(16)	96.44(13)	96.03(13)	96.27(15)
OA-Al1-OB	177.97(17)	177.82(15)	177.4(2)	177.33(14)	177.9(3)	177.0(3)	176.82(16)	176.22(18)
OD-Al1-OA	88.76(17)	89.10(13)	89.47(19)	89.45(12)	89.2(3)	89.60(18)	89.64(15)	89.52(16)
OD-Al1-OA	90.57(16)	90.33(14)	90.19(19)	90.00(12)	90.2(3)	89.99(19)	89.74(15)	89.93(16)
OD-Al1-OB	92.05(16)	91.89(14)	92.14(18)	92.31(12)	92.1(3)	92.69(18)	92.94(14)	93.36(16)
OD-Al1-OB	88.64(17)	88.7(14)	88.22(18)	88.25(12)	88.4(3)	87.73(18)	87.70(14)	87.22(17)
QE*	1.01	1.01	1.01	1.01	1.01	1.01	1.01	1.01
AV†	18.36	17.43	18.11	17.34	17.13	17.83	16.20	18.15
Al2-OA	1.822(3)	1.811(3)	1.811(3)	1.806(2)	1.808(4)	1.805(3)	1.788(5)	1.788(4)
Al2-OC	1.889(3)	1.888(3)	1.885(3)	1.884(2)	1.880(4)	1.870(3)	1.870(4)	1.854(4)
Al2-OC	1.831(6)	1.821(5)	1.837(7)	1.816(4)	1.83(1)	1.821(8)	1.812(4)	1.808(4)
Al2-OD (x2)	1.820(3)	1.808(2)	1.804(3)	1.804(2)	1.804(4)	1.795(3)	1.792(2)	1.786(3)
AVG.	1.84	1.83	1.83	1.82	1.82	1.82	1.81	1.80
Poly. Vol.	5.16(5)	5.08(4)	5.09(5)	5.04(3)	5.06(7)	5.00(6)	4.95(5)	4.90(5)
OC-Al2-OC	73.4(3)	73.7(2)	74.4(3)	73.92(19)	74.7(4)	74.4(3)	74.6(2)	74.4(2)
OC-Al2-OA	160.5(4)	160.7(3)	161.5(4)	161.00(3)	161.4(6)	161.2(4)	161.40(18)	161.7(2)
OC-Al2-OA	87.05(19)	87.03(17)	87.0(3)	87.05(15)	86.7(3)	86.8(3)	86.78(19)	87.3(2)
OD-Al2-OD	105.7(2)	106.04(19)	105.9(3)	106.09(18)	105.7(3)	106.2(3)	106.44(16)	106.4(2)
OA-Al2-OD	98.88(13)	99.08(11)	99.15(15)	99.11(10)	99.2(2)	99.27(15)	99.48(13)	99.49(13)
Si-OB	1.641(6)	1.639(4)	1.641(6)	1.636(4)	1.622(8)	1.629(6)	1.625(4)	1.625(5)
Si-OC	1.629(5)	1.623(4)	1.607(6)	1.616(4)	1.606(8)	1.610(6)	1.603(4)	1.609(4)
Si-OD (x2)	1.628(2)	1.6292(17)	1.630(2)	1.6277(15)	1.625(2)	1.625(2)	1.617(3)	1.614(3)
AVG.	1.63	1.63	1.63	1.63	1.62	1.62	1.62	1.62
Poly. Vol.	2.22(3)	2.21(2)	2.20(3)	2.198(18)	2.17(3)	2.18(3)	2.15(2)	2.15(2)
OB-Si-OC	102.0(2)	101.82(18)	101.4(3)	102.10(16)	101.2(4)	101.8(3)	101.8(2)	101.5(2)
OD-Si-OD	109.15(16)	109.17(12)	109.23(14)	108.94(11)	109.27(17)	108.98(16)	108.67(11)	109.0(2)
OD-Si-OC	110.88(18)	111.22(12)	111.28(19)	111.12(13)	111.0(2)	111.04(18	111.26(12)	111.19(14)
QE*	1.00	1.00	1.00	1.00	1.00	1.00	1.00	1.00
AV†	14.30	14.85	16.30	14.05	17.41	15.20	15.44	16.50
OA-OB	2.779(7)	2.772(7)	2.7687(15)	2.7671(11)	2.7635(17)	2.759(2)	2.7522(2)	2.745(2)
OB-OB	2.471(7)	2.466(6)	2.461(7)	2.467(5)	2.474(10)	2.468(7)	2.479(8)	2.465(9)
OA-OA	2.468(7)	2.475(6)	2.468(8)	2.476(5)	2.458(10)	2.462(8)	2.474(8)	2.458(8)
Al1′-Al1′	2.686(3)	2.8614(19)	2.862(2)	2.8569(16)	2.853(3)	2.850(3)	2.841(3)	2.834(3)
Al1-Al1	2.686(3)	2.6835(19)	2.674(2)	2.6760(16)	2.674(3)	2.666(3)	2.661(3)	2.653(3)
OD-OD	4.153(7)	4.138(5)	4.112(8)	4.101(5)	4.084(9)	4.063(8)	4.033(5)	4.006(6)
Al1-OD-Al2	121.55(15)	121.78(11)	122.09(14)	121.92(9)	122.09(17)	122.09(14)	122.08(14)	122.20(16)
Al1-OD-Si	111.74(18)	111.20(13)	111.2(2)	111.38(13)	111.6(2)	111.52(18)	111.49(13)	111.65(16)
Al2-OD-Si	126.0(2)	126.14(16)	125.8(2)	125.78(25)	125.5(3)	125.5(2)	125.37(17)	125.1(2)
Al2-OC-Al2	106.6(3)	106.3(2)	105.6(3)	106.08(19)	105.3(4)	105.6(3)	105.4(2)	105.6(2)

* Quadratic elongation.
† Angle variance.

TABLE 9. Selected bond lengths (Å) and angles (°) for sillimanite at room pressure through 7.663 GPa

Bond or Angle	Pressure (GPa)				
	0.0001	1.548(5)	4.144(7)	5.750(7)	7.663(8)
Al1-OA (x2)	1.916(3)	1.914(4)	1.893(5)	1.868(5)	1.867(5)
Al1-OB (x2)	1.863(3)	1.865(4)	1.855(4)	1.840(4)	1.838(4)
Al1-OD (x2)	1.954(7)	1.943(9)	1.914(9)	1.889(9)	1.887(9)
Avg.	1.91	1.91	1.89	1.87	1.86
Poly. Vol	9.15(11)	9.11(14)	8.81(13)	8.46(14)	8.47(13)
OA-Al1-OB	99.85(19)	99.6(3)	100.4(3)	101.8(3)	101.4(2)
OA-Al1-OB′	80.15(19)	80.4(3)	79.6(3)	78.2(3)	78.6(2)
OA-Al1-OD	88.4(2)	88.0(3)	88.8(3)	90.3(4)	89.7(3)
OA-Al1-OD′	91.6(2)	92.0(3)	91.2(3)	89.7(4)	90.2(3)
OB-Al1-OD	90.4(3)	90.4(3)	91.3(4)	93.5(4)	92.8(4)
OB-Al1-OD′	89.6(3)	89.6(3)	88.8(4)	86.5(4)	87.2(4)
QE*	1.01	1.01	1.01	1.02	1.02
AV†	36.27	35.26	40.45	54.91	50.67
Al2-OB	1.753(5)	1.742(6)	1.749(6)	1.782(7)	1.764(7)
Al2-OC	1.706(7)	1.698(8)	1.699(9)	1.712(9)	1.7114(11)
Al2-OD (x2)	1.798(5)	1.789(6)	1.785(6)	1.781(8)	1.773(7)
Avg.	1.76	1.75	1.75	1.76	1.76
Poly. Vol	2.79(5)	2.75(5)	2.75(6)	2.79(7)	2.75(7)
OB-Al2-OC	113.5(5)	113.6(5)	112.2(5)	108.9(5)	110.3(5)
OB-Al2-OD	105.45(18)	105.3(2)	105.6(2)	106.3(2)	105.6(2)
OC-Al2-OD	108.06(18)	107.9(2)	108.2(2)	108.8(3)	109.0(2)
OD-Al2-OD′	116.5(5)	116.9(7)	117.3(6)	117.5(8)	117.2(7)
QE*	1.01	1.01	1.01	1.00	1.01
AV†	20.46	22.30	20.49	17.04	18.67
Si-OA	1.635(4)	1.626(5)	1.636(5)	1.656(6)	1.643(6)
Si-OC	1.572(8)	1.572(9)	1.590(10)	1.588(10)	1.569(12)
Si-OD (x2)	1.642(5)	1.645(7)	1.632(6)	1.635(7)	1.629(7)
Avg.	1.62	1.62	1.62	1.63	1.62
Poly. Vol	2.19(4)	2.19(5)	2.19(5)	2.22(5)	2.18(6)
OA-Si-OC	109.8(5)	110.3(6)	108.0(6)	106.0(6)	106.6(5)
OA-Si-OD	106.93(19)	106.6(3)	107.4(3)	108.2(3)	107.7(2)
OC-Si-OD	110.9(2)	111.2(3)	111.3(3)	111.8(3)	111.8(4)
OD-Si-OD′	111.2(5)	110.9(7)	111.3(7)	110.7(8)	111.2(7)
QE*	1.00	1.00	1.00	1.00	1.00
AV†	4.05	5.02	4.09	5.65	5.72
OA-OB	2.892(8)	2.888(9)	2.8800(11)	2.8775(16)	2.8665(15)
OA-OB	2.433(8)	2.439(10)	2.400(10)	2.340(11)	2.347(10)
Al1-Al1	2.884(0)	2.879(0)	2.871(0)	2.867(0)	2.857(0)
OD-OD	3.907(15)	3.886(18)	3.828(17)	3.777(19)	3.775(18)
Al1-OA-Si	129.26(9)	128.96(12)	128.93(11)	128.85(9)	128.77(10)
Al1-OB-Al2	129.00(15)	129.46(11)	129.30(14)	128.6(2)	128.93(19)
Al2-OC-Si	171.3(6)	171.0(5)	170.5(5)	170.8(6)	170.7(7)
Al1-OD-Al2	116.7(3)	116.6(3)	116.1(3)	115.6(3)	115.7(3)
Al1-OD-Si	125.3(3)	125.5(3)	125.4(3)	125.5(3)	125.1(3)
Al2-OD-Si	114.1(6)	114.0(7)	114.4(6)	114.2(7)	114.3(7)
OB-OA-OB	88.38(11)	88.50(12)	88.83(14)	89.11(18)	89.11(18)

* Quadratic elongation.
† Angle variance.

fits: χ^2_w doubles to 5.79 with a calculated K_{T0} of 167.7(5) for sillimanite and χ^2_w increases to 30.53 with a calculated K_{T0} of 154(1) for andalusite. In addition, the largest difference between the observed and calculated pressures increases to 0.05 GPa for sillimanite and 0.23 GPa for andalusite. The improvements in the determination of K_{T0} and K' for andalusite and sillimanite are achieved by improvements in peak-fitting algorithms and the use of quartz as an internal pressure standard (e.g., Angel 2001). The use of quartz as an internal pressure standard improves the precision of σ_p from 0.05 GPa to typically less than 0.01 GPa, which leads to a threefold reduction in the uncertainty of the bulk modulus. Further improvements to the uncertainties are achieved by increasing the pressure range of the experiments while maintaining the precision of the pressure.

The variation of the unit-cell axes of sillimanite and andalusite with pressure also display significant curvature (Fig. 4). We therefore determined the axial moduli using a parameterized form of the third-order Birch-Murnaghan equation for volume using

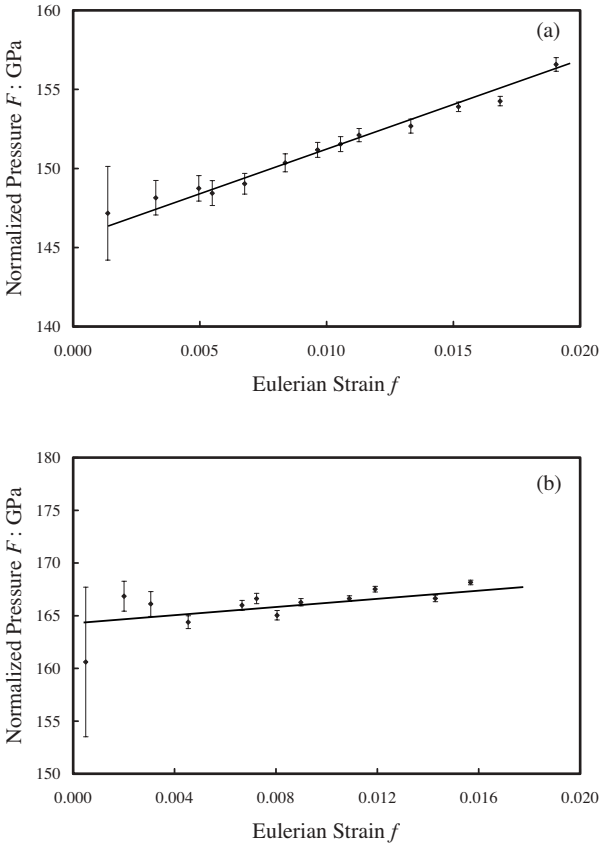

FIGURE 3. Variation of the normalized pressure, F, against the Eulerian strain, f, for (**a**) andalusite and (**b**) sillimanite.

the EosFit 5.2 program (Angel 2001) in which the individual axes are cubed. Results of this analysis yield values of K_{a_0} = 163(1) GPa, K_{b_0} = 113.1(7) GPa, and K_{c_0} = 297(1) GPa with K'_{a_0} = 2.1(3), K'_{b_0} = 5.1(2), and K'_{c_0} = 11.1(4) for sillimanite, and K_{a_0} = 99.6(7) GPa, K_{b_0} = 152.2(9) GPa, and K_{c_0} = 236(3) GPa with K'_{a_0} = 5.8(2), K'_{b_0} = 7.6(3), and K'_{c_0} = 5.5(9) for andalusite. Thus c is the least compressible parameter in both structures. The compression of the two structures is anisotropic with a maximum anisotropy in sillimanite of ~61% (c to b) and ~58% (c to a) in andalusite. There is a 31% difference in compression between the a and b parameters of sillimanite and a ~35% difference in compression between the a and b parameters of andalusite. The difference in K' of the axes is shown in Figure 5, which represents the nonlinear nature of the axial compressibilities. The K' of andalusite, 6.8(2), can be attributed to axial compressibilities that range from K'_{c_0} = 5.5 to K'_{b_0} = 7.6(3). In contrast with andalusite, sillimanite shows a greater range where the highest value is found along c, K'_{c_0} = 11.1(4), and the smallest value is found along a, K'_{a_0} = 2.1(3). The latter is responsible for the lower K' of sillimanite compared with andalusite. In addition, the axial compressibilities determined in this study indicate that the compression anisotropy of sillimanite (β_a:β_b:β_c = 1/K_a:1/K_b:1/K_c = 1.82:2.63:1.00) is slightly greater than that of andalusite (β_a:β_b:β_c = 1/K_a:1/K_b:1/K_c 2.37:1.55:1.00). The values for andalusite are in reasonable agreement with the linear axial compressibilities determined by Ralph et al. (1984) (β_a:β_b:β_c = 2.13:1.47:1.00). Yang et al. (1997)

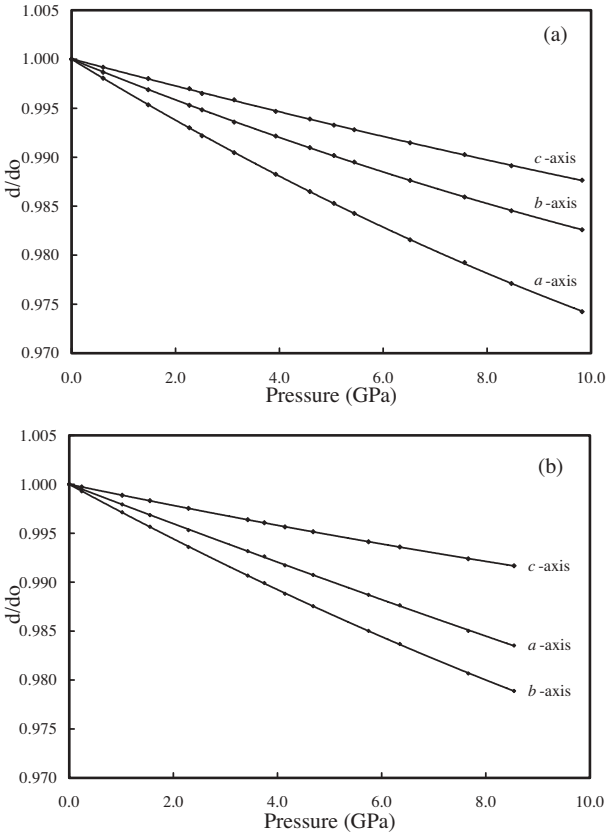

FIGURE 4. Variations of axial lengths with pressure for (**a**) andalusite and (**b**) sillimanite.

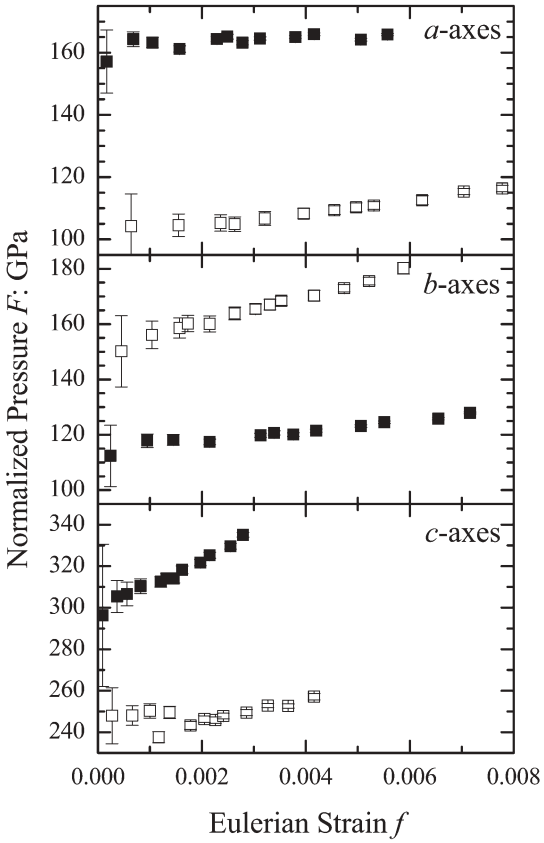

FIGURE 5. Variation of the normalized pressure, *F*, against the Eulerian strain, *f*, for the individual axes in andalusite (white squares) and sillimanite (black squares).

reported values for sillimanite at room pressure (β_a:β_b:β_c = 1.22:1.63:1.00) and noted that they changed significantly at 5.29 GPa (β_a:β_b:β_c = 4.07:5.43:1.00) due to the nonlinear nature in the axial compressibilities. However, linear compressibilities determined over the entire pressure range from the axial length vs. pressure data of Yang et al. (1997), β_a:β_b:β_c = 1.93:2.62:1.00, are in good agreement with this study.

The main compression mechanism within both structures is the reduction of bond lengths within the polyhedra. In both andalusite and sillimanite, the [Al1O_6] octahedron is the most compressible unit in the structure as a result of the shortening of the Al1-OD bond, the longest bond in the octahedron. In andalusite, the Al1-OD bond decreases from 2.076(3) to 2.003(3) Å (~3.5%) between 1 bar and 9.8 GPa while Al1-OB decreases by ~0.8% and Al1-OA, the shortest bond, decreases by ~0.9% (Table 8). Overall, the volume of the octahedron decreases by ~5.1%. Within the [Al2O_5] trigonal bipyramid, all of the bond lengths decrease within the pressure range examined by ~1.9% except the Al2-OC bond in the (010) plane, which decreases by ~1.3% resulting in an overall decrease in volume of ~5.0%. Within the SiO_4 tetrahedra, all bonds decrease between 1 bar and 9.8 GPa by ~1.0% resulting in a decrease in the volume of ~3.2%. In the [Al1O_6] octahedron of sillimanite, all Al-O bonds decrease with increasing pressure. The longest bond, Al1-OD, is the most compressible, decreasing by ~3.4%, while the Al1-OA bond decreases by ~2.6% and the Al1-OB bond decreases ~1.4% between 1 bar and 7.6 GPa. Overall, the volume of the octahedron decreases by ~7.4%. The [Al2O_4] and [SiO_4] tetrahedra in sillimanite behave as rigid units and show no significant change throughout the pressure range examined (Table 8). The incompressibility of the [Al2O_4] and [SiO_4] tetrahedron is in contrast to the results of Yang et al.'s (1997) study where they observed a decrease in the volume of both tetrahedra. This apparent discrepancy is the consequence of differences in calculation of the estimated standard deviations of the polyhedral volumes. We used estimated standard deviations from the bond lengths to recalculate the maximum possible standard deviations in the polyhedral volumes.

The compression anisotropy of andalusite and sillimanite can, in large part, be attributed to the compression of the Al-O bonds within the [Al1O_6] octahedron. In both structures, the [Al1O_6] octahedron share edges and run parallel to *c*, which is the least compressible axis in both structures. Orientation of the octahedra within the (001) plane is shown in Figure 1 and determines which axial direction is the most compressible. The most compressible axis corresponds to the direction of the most compressible bond (Al1-OD) within the octahedra. The Al1-OD bond is located ~30° from *b* in sillimanite and ~30° from *a* in andalusite. The [AlO_6] octahedra in sillimanite rotate from 29.45(4)° to 30.66(6)° with respect to *b*, while the rotation in andalusite changes from 30.33(4)° to 29.32(7)° with respect to *a*. The role of the orientation of the [Al1O_6] octahedra in deter-

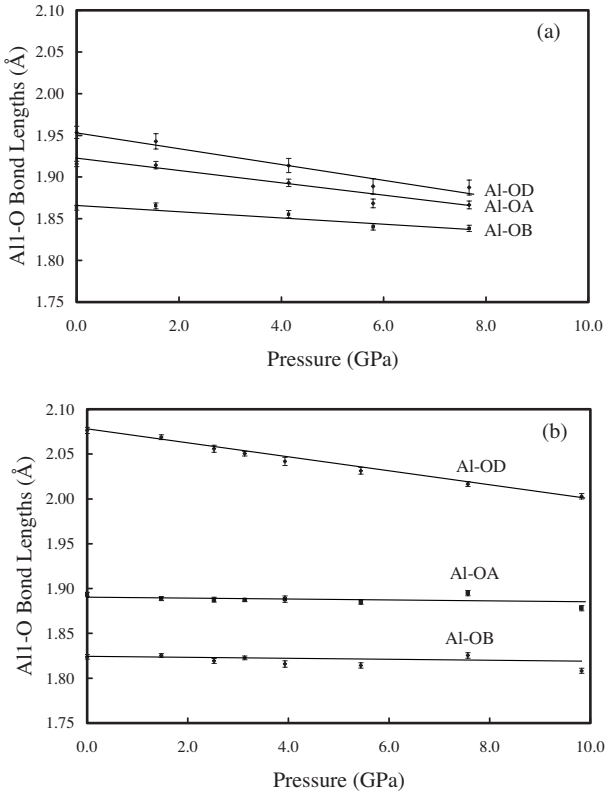

FIGURE 6. The variation of octahedral Al1-O bond distances in (**a**) sillimanite and (**b**) andalusite.

mining the relative axial compressibilities has been previously noted by Ralph et al. (1984), Vaughan and Weidner (1978), and Yang et al. (1997).

The aluminum octahedra in andalusite and sillimanite are the most compressible polyhedra in their structures, but the effect of pressure on the octahedra is different in each, as seen in the decrease in the bond lengths and volumes of the octahedra. The only major compression in the [Al1O_6] octahedron of andalusite is along the Al-OD bond, while there is significant compression along all of the bonds within the [Al1O_6] octahedron of sillimanite (Fig. 6). Shortening of the OA-OB distance perpendicular to [100] in sillimanite results in a change in the OA-Al1-OB angles and is reflected in a change of the angle variance (Robinson et al. 1971) from 36.27 to 50.67 between 1bar and 7.66 GPa. Thus, due to a greater amount of axial shortening and bond bending the overall compression of the aluminum octahedron in sillimanite, ~7.4%, is much greater than that in andalusite, ~3.6%, between 1 bar and 7.6 GPa. The greater change in the octahedral volume in sillimanite is also due to the compression of all Al-O bonds (Fig. 6a) compared with andalusite where there is compression only along the Al-OD bond (Fig. 6b). We suggest that the incompressibility of the Al-OA and Al-OB bonds in andalusite may be due to the compressibility of the [Al2O_5] and [SiO_4] polyhedra. This is in contrast with sillimanite where all of the Al-O bonds in the octahedra are compressible while the [Al2O_4] and [SiO_4] polyhedra are incompressible. Thus, there seems to be a relationship between the compressibility or incompressibility of the polyhedra surrounding the octahedra in andalusite and sillimanite and the compressibility or incompressibility of the Al-OA and Al-OB bonds within the octahedra.

ACKNOWLEDGMENTS

J.B. Burt gratefully acknowledges support from NSF grant EAR-0229472. This work was also supported by a fellowship awarded to M. Koch from the DAAD.

REFERENCES CITED

Angel, R.J. (2001) Equations of state. In R.M. Hazen and R.T. Downs, Eds., High-Temperature and High-Pressure Crystal Chemistry, 41, 35–60. Reviews in Mineralogy and Geochemistry, Mineralogical Society of America, Chantilly, Virginia.

——— (2003) Automated profile analysis for single-crystal diffraction data. Journal of Applied Crystallography, 36, 295–300.

——— (2004) Absorption corrections for diamond-anvil cells implemented in the software package Absorb 6.0. Journal of Applied Crystallography, 37, 486–492.

Angel, R.J., Allan, D.R., Miletich, R., and Finger, L.W. (1997) The use of quartz as an internal pressure standard in high-pressure crystallography. Journal of Applied Crystallography, 30, 461–466.

Burnham, C.W. (1966) Computation of absorption corrections and the significance of end effects. American Mineralogist, 51, 159–167.

Creagh, D.C. and McAuley, W.J. (1992) X-ray dispersion correction. In A.J.C. Wilson, Ed., International tables for crystallography, vol. C, 206–219. Kluwer Academic Publishers, Dordrecht.

Finger, L.W. and Prince, E. (1974) A system of Fortran IV computer programs for crystal structure computations. U.S. National Bureau of Standards Technical Note 854.

Friedrich, A., Kunz, M., Winkler, B., and Le Bihan, T. (2004) High-pressure behavior of sillimanite and kyanite: compressibility, decomposition and indications of a new high-pressure phase. Zeitschrift für Kristallographie, 219, 324–329.

Hazen, R.M., Downs, R.T., and Prewitt, C.T. (2000) Principles of comparative crystal chemistry, high-temperature and high-pressure crystal chemistry. In R.M. Hazen and R.T. Downs, Eds., High-Temperature and High-Pressure Crystal Chemistry, 41, 1–30. Reviews in Mineralogy and Geochemistry, Mineralogical Society of America, Chantilly, Virginia.

Kerrick, D.M. (1990) Metamorphic reactions. In D.M. Kerrick, Ed., The Al_2SiO_5 polymorphs. 22, 223–253. Reviews in Mineralogy, Mineralogical Society of America, Chantilly, Virginia.

King, H.E. and Finger, L.W. (1979) Diffracted beam crystal centering and its application to high-pressure crystallography. Journal of Applied Crystallography, 12, 374–378.

Maslen, E.N., Fox, A.G., and O'Keefe, M.A. (1992) X-ray scattering. In A.J.C. Wilson, Ed., International Tables for Crystallography, vol. C, 476–509. Kluwer Academic Publishers, Dordrecht.

Matsui, M. (1996) Molecular dynamics study of the structures and bulk moduli of crystals in the system CaO-MgO-Al_2O_3-SiO_2. Physics and Chemistry of Minerals, 23, 345–353.

Miletich, R., Allan, D.R, and Kuhs W.F. (2000) High-pressure single crystal techniques. In R.M. Hazen and R.T. Downs, Eds., High-Temperature and High-Pressure Crystal Chemistry. 41, 445–519. Reviews in Mineralogy and Geochemistry, Mineralogical Society of America, Chantilly, Virginia.

Oganov, A.R., Price, D.G., and Brodholt, J.P. (2001) Theoretical investigation of metastable Al_2SiO_5 polymorphs. Acta Crystallographica, A57, 548–557.

Orear, J. (1982) Least-squares when both variables have uncertainties. American Journal of Physics, 50, 912–916.

Pavese, A. and Artioli, G. (1996) Profile-fitting treatment of single-crystal diffraction data. Acta Crystallographica, A52, 890–897.

Ralph, R.L., Finger, L.W., Hazen, R.M., and Ghose, S. (1984) Compressibility and crystal structure of andalusite at high pressure. American Mineralogist, 69, 513–519.

Robinson, K., Gibbs, G.V., and Ribbe, P.H. (1971) Quadratic elongation: A quantitative measure of distortion in coordination polyhedra. Science, 172, 567–570.

Vaughan, M.T. and Weidner, D.J. (1978) The relationship of elasticity and crystal structure in andalusite and sillimanite. Physics and Chemistry of Minerals, 3, 133–144.

Winkler, B., Hytha, M., Warren, M.C., Milman, V., Gale, J.D., and Schreuer, J. (2001) Calculation of the elastic constants of the Al_2SiO_5 polymorphs andalusite, sillimanite, and kyanite. Zeitschrift für Kristallographie, 216, 67–70.

Winter, J.K. and Ghose, S. (1979) Thermal expansion and high-temperature crystal chemistry of the Al_2SiO_5 polymorphs. American Mineralogist, 64, 573–586.

Yang, H., Hazen, R.M., Finger, L.W., Prewitt, C.T., and Downs, R.T. (1997) Compressibility and crystal structure of sillimanite, Al_2SiO_5, at high pressure. Physics and Chemistry of Minerals, 25, 39–47.

MANUSCRIPT RECEIVED DECEMBER 8, 2004
MANUSCRIPT ACCEPTED MAY 12, 2005
MANUSCRIPT HANDLED BY GEORGE LAGER